INTERNATIONAL JOURNAL OF LATEST TECHNOLOGY IN ENGINEERING, MANAGEMENT & APPLIED SCIENCE (IJLTEMAS)

ISSN 2278-2540 | DOI: 10.51583/IJLTEMAS | Volume XV, Issue I, January 2026

Performance of Strut-Free Retaining Walls for 30 M Deep Excavations in Soft Clay

Bashir Osman[1*], Abdelrahman Abuserriya[2]

Department of Civil Engineering, Engineering College, Sinnar University, Sinnar, Sudan

***Corresponding Author**

DOI: https://doi.org/10.51583/IJLTEMAS.2026.150100056

Received: 16 January 2026; Accepted: 26 January 2026; Published: 06 February 2026

ABSTRACT

Strut-free retaining wall systems offer important advantages for deep excavations, including improved construction efficiency, safety, and workspace availability. However, their application in excavations deeper than 20 m in soft clay remains limited. This study investigates the deformation behavior and optimal design parameters of a strut-free retaining wall system for a 30 m deep excavation in soft clay using three-dimensional finite element analysis. The retaining system consists of diaphragm walls, buttress walls, cross walls, and rib walls. A total of sixty-one numerical simulations were conducted to evaluate the influence of the number, thickness, and height of buttress and cross walls on wall deflection and ground settlement. The Hardening Soil model was adopted to represent the nonlinear behavior of soft clay, while structural components were modeled as elastic plate elements. The results indicate that increasing the number of buttress walls in the long excavation direction significantly reduces maximum wall deflection and surface settlement, whereas the effect in the short direction is relatively small. Among the investigated layouts, the configuration with two rib walls in the long direction and one in the short direction provided the most effective deformation control.

Keywords: Strut-free retaining wall; Deep excavation; Soft clay; Buttress wall; Ground settlement; Finite element analysis

INTRODUCTION

A strut-free retaining wall system is new system to support the deep excavation and it was studied in different occasion [1-10]. The design of retaining wall supports excavation has to be aware of many things: firstly, the vertical movement and safety of machines and workers. Secondly, the dimensions of excavation. Thirdly, water and soil condition and fourthly, the force and load acting on the retaining wall. The advantages of a strut-free retaining wall system include a wide construction space, enhanced excavation process and reduced time and cost.

Zheng, et al. [11] presented A new strut-free retaining wall system, referred to as an inclined-vertical framed retaining wall (IVFRW) for excavation in clay. They designed and established the previous system in China. The excavation dimension is 80 m wide, 110 m long and 4.9 m deep. The diaphragm wall is 0.6 m thick and 12 m long. The inclined pile is 0.6 m thick, 12 m long and the inclination angle 20 degrees and the capping beam is 0.423 m thick and 1 m wide. They used PLAXIS 3D to simulate IVFRW system and the hardening soil model and Mohr-Coulomb to model the soil stress distribution and interface between soil and system structure respectively. The soil strength reduction is equal to 0.67. The maximum wall deflection is 0.56% H, which is less than 0.8% as reported in previous studies [12-14]. They made a parametric study to understand the mechanism and performance of IVFRW. The results show that the wall deflection decreased when the inclined pile length increased. In contrast, the increasing length of the vertical diaphragm wall changed the computed vertical wall deflections and surface ground settlements.

Zheng, et al. [15] presented A new strut-free retaining wall system, referred to as an outward inclined-vertical framed retaining wall (OIVFRW) for excavation in clay. They designed and established the previous system in China. The excavation area is 23000 m^2 and 5.7 m deep. The diaphragm wall is 0.5 m thick and 11 m long.

ISSN 2278-2540 | DOI: 10.51583/IJLTEMAS | Volume XV, Issue I, January 2026

The inclined pile is 0.5 m thick, 10 m long and the inclination angle 18 degrees and the capping beam is 0.423 m thick and 1 m wide. They used PLAXIS 3D to simulate the OIVFRW system and the Hardening soil model and Mohr-Coulomb to model the soil stress distribution and interface between soil and system structure, respectively. The soil strength reduction is equal 0.67. The maximum wall deflection is 0.41% H, which is less than 0.8%. They made a parametric study to understand the mechanism and performance of OIVFRW. The results show that the wall deflection and surface ground settlement decreased when the inclined pile length increased. In the past, most of excavation systems deep were between 5 m to 20 m and around 8 cases or 10 cases over 20 m [16]. Today, Tan, et al. [17] presented a statistical analysis of 592 deep excavation cases history in Shanghai from 1995 to 2018 and they found 14% of cases over 20 m in Shanghai only. The required for new system for deep excavation over 20 m is essential and vital to continue progress in deep excavation system technology. This paper aims to find the effective range of dimension of buttress walls, rib walls and cross walls and select the optimum design between three different designs in terms of minimizing the maximum wall deflection and ground settlement for a strut-free retaining wall system which has 30 m deep in soft clay.

METHODOLOGY

Model geometry, mesh, and boundary condition

The geometry of the excavation was assumed to be 150 m long, 75 m wide and 30 m deep. The model was divided in two parts because it is symmetrical in two axes (x and y axes) and to minimize the time of program analysis. The final excavation depth (H) was 30 m, and the height of the diaphragm wall was assumed to be 50 m. The cross walls and rib wall are located directly under the excavation level. The distance between the diaphragm walls and the outer boundary of the mesh was larger six times the final excavation depth [18, 19], which is 195 m to minimize the boundary effect and the depth of the model is 70 m. So, the model geometry is 465 m long, 285 m wide and 70 m deep.

The thickness of a diaphragm wall can be assumed to be 5% H in the preliminary design, where H is the final excavation depth [20], so the diaphragm wall thickness is 1 m instead of 1.5 m because of excessive movements were deliberately designed for this study. The mesh of the model is very fine as shown in Figure 1.

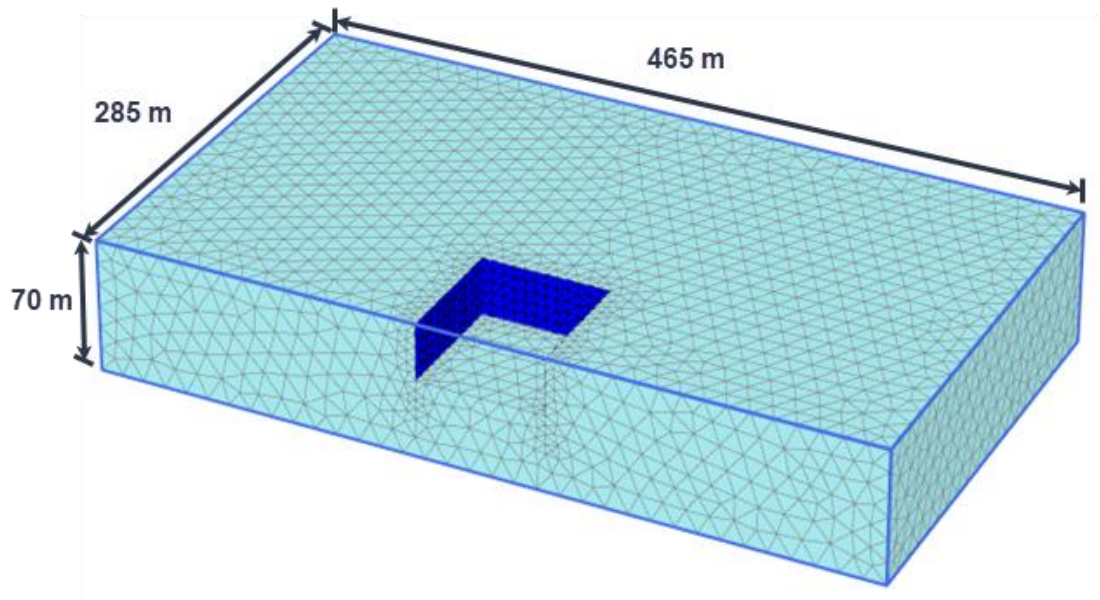

Figure 1: Typical geometry and finite element mesh used for analysis

Estimation of soil parameters

A 10-node tetrahedral element simulated the soil volume, and the suitable soil model for soft clay is the hardening soil (HS) model [21] to simulate the settlement and deformation of soil.

ISSN 2278-2540 | DOI: 10.51583/IJLTEMAS | Volume XV, Issue I, January 2026

The hardening soil model simulates the soft clay soil around the retaining system. The hardening soil model needs 11 parameters, which are unsaturated unit weight which equals 20 kPa, effective cohesion (c) which equals 0 , effective angle of internal friction (φ) which equals 30 [22], angle of dilatancy (ψ) which equals 0 [23], secant referential stiffness (E_{50}^{ref}) which equals 9488 kPa [22], tangent referential stiffness for primary oedometer loading (E_{oed}^{ref}) which equals 6642 kPa [22], unloading/reloading referential stiffness (E_{ur}^{ref}) which equals 28470 kPa [24], power for stress-level dependency of stiffness (m) which equals 1, Poisson's ratio for unloading–reloading (υ_{ur}) which equals 0.2, reference stress for stiffness (p^{ref}) which equals 100 kPa, value for normal consolidation (K_0^{nc}) which equals 0.5, failure ratio (R_f) which equals 0.9 [21, 25]. The input parameters of the soil were typical values for Taipei silty clay (CL) and were obtained from Lim, et al. [26]. These parameters are calibrated and validated through two case histories [27].

Estimation of structural element parameters

A 6-noded isotropic-elastic-plate element was applied to model the retaining wall system structural members, such as diaphragm walls, cross walls, rib-walls and buttress walls as elastic behavior. Also, the same element was applied as to model the elastoplastic behavior and the elastic-plate element is used to simulate the concrete in the retaining system. The elastic model of the plate needs eight parameters which are thickness (d), unit weight (γ) which equals 25 kN/m^3, Young's modulus in first axial direction (E_1) which equals 19,717,606 kPa [28], Young's modulus in second axial direction (E_2), in-plane shear modulus (G_{12}) which equals 8,215,670 kPa [29], Out-of-plane shear modulus related to shear deformation over first direction (G_{13}), Out-of-plane shear modulus related to shear deformation over second direction (G_{23}) and Poisson's ratio (υ_{12}) which equals 0.2 [29]. As the material is Isotropic so, $E_1 = E_2$ and $G_{12} = G_{13} = G_{13}$. The compressive strength of concrete ($\grave{f}_c$) is assumed to be 27.45 MPa and According to the American Concrete Institute ACI 318-19 [28] code, the nominal value of Young's modulus for concrete can be estimated by using equation $E = 4700\sqrt{\grave{f}_c}$. The stiffness of the structural element was reduced by 20% from its nominal value because of the probability of the occurrence of cracks in concrete resulting from the large bending moment of the diaphragm [30].

The interface element described the soil-structure interaction. If the relationship between structure and soil is frictional so, the strength reduction factor (R_{inter}) is equal to 1. Also, if the soil-structure interaction is frictionless or weak frictional, then the strength reduction factor (R_{inter}) is less than 1. In this research will used R_{inter} equal 1.

Select the height of stage excavation

The retaining wall system is constructed and excavated in many stages: the first stage is the installation of retaining wall system structural members and the second stage is excavation of the entire soil. The soil was excavated sequentially, and the groundwater level was assumed to be under the final excavation surface ground so it would not affect the retaining system. Also, the excavation scenario is conducted at several excavation heights and different mesh coarseness, and Table 1 shows the maximum wall deflection for every trial in both directions for different excavation heights and mesh coarseness.

Table 1: Maximum wall deflection for every trial in both directions for different excavation heights and mesh coarseness

Direction	Long direction			Short direction		
	Mesh coarseness			Mesh coarseness		
Excavation height (m)	Very coarse (m)	Medium coarse (m)	Very fine (m)	Very coarse (m)	Medium coarse (m)	Very fine (m)
3	8.34	7.857	8.736	1.545	1.591	1.56
4	7.12	6.565	8.32	1.39	1.269	1.49
6	6.183	7.183	8.369	1.15	1.106	1.55

ISSN 2278-2540 | DOI: 10.51583/IJLTEMAS | Volume XV, Issue I, January 2026

According to Table 1, the excavation height of 6 m is chosen with very fine mesh because it is similar to the 3 m excavation height and very fine mesh to minimize the calculation time.

The retaining wall system design

The retaining wall system comprises four main parts: diaphragm walls, rib walls, cross walls, and buttress walls
as described in previous study [26]. The schematic diagram of the plan view of the Rigid and Fixed Diaphragm (RFD) wall retaining system in Figure 2 and Figure 3 shows the schematic diagram of part of plan view and cross section of the RFD system wall.

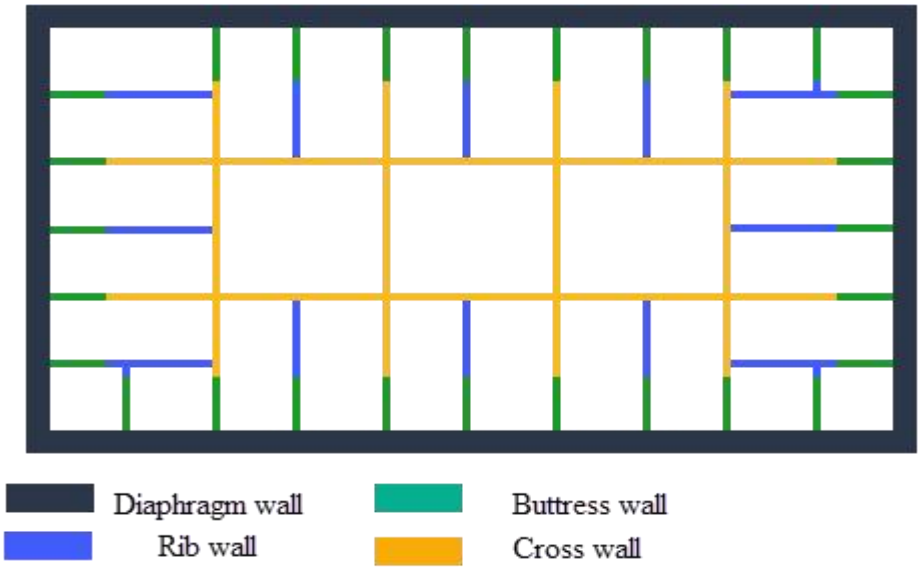

Figure 2: The schematic diagram of plan view of the RFD system wall

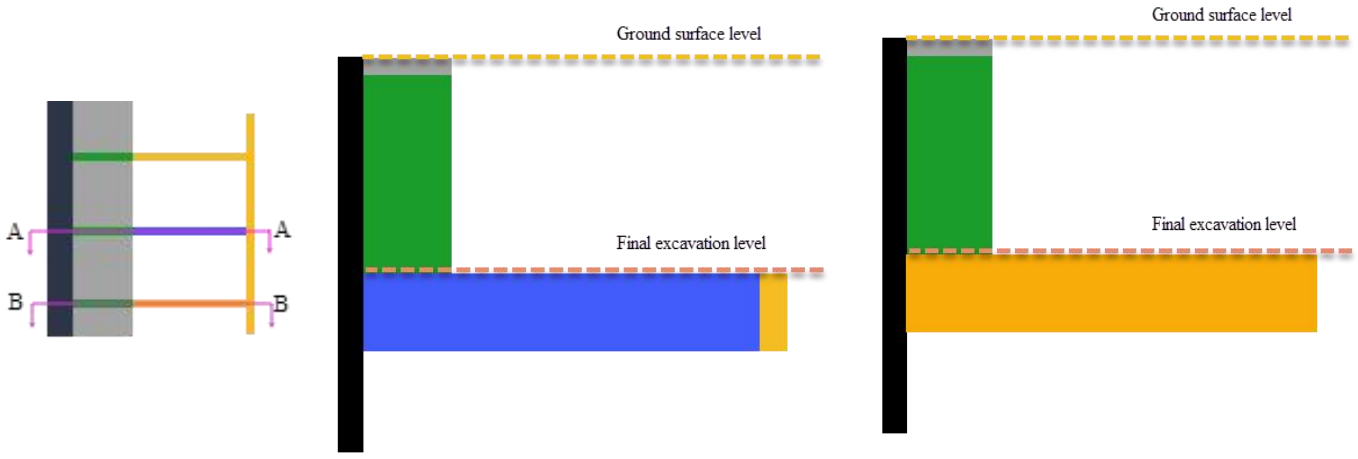

(a) (b) (c)

Figure 3: The schematic diagram of the RFD system wall: a) part of plan view, b) cross section A-A, c) cross section B-B

Parametric study.

Four series of simulations were conducted to understand the performance and mechanism of the integrated retaining system as listed in Table 2. For each series, the thickness of diaphragm walls is constant at 1 m. The first series was conducted as the basic analysis for finding the optimum number of buttress and cross wall to

ISSN 2278-2540 | DOI: 10.51583/IJLTEMAS | Volume XV, Issue I, January 2026

minimize the wall deflection and surface ground settlement. The buttress walls arrangement was uniformly distributed along both sides of the diaphragm wall. Also, the second and third series of scenarios are conducted to find the optimum thickness and height of buttress wall. The fourth series is investigated to find the optimum height of the cross wall and rib wall. Three designs were used to find the optimum design in series 1. The first is one rib wall before every cross wall, as shown in Figure 4(a) in both directions, the second is two rib walls before every cross wall as shown in Figure 4(b) in both directions and the third is two rib walls before every cross wall in long direction and one rib wall before every cross wall in short direction as shown in Figure 4(c).

In total, 61 numerical runs were conducted to investigate to select the optimum design (series 1). As mentioned before, there are 45 runs for the first type of design (type 1), eight runs for the second type of design (type 2) and eight runs for the third type of design (type 3).

Table 2: List of simulation programs for design consideration of buttress walls

Series	Number of buttress wall (N_{bw})	Direction	Number of cross wall (N_{cw})	Thickness of buttress wall and cross wall (t_{bw}) (m)	Hight of buttress wall (H_{bw}) (m)	Hight of cross wall (H_{cw}) (m)	Existence of rib wall
1-type 1	5, 9, 13, 17, 21, 25, 29, 33, 37	Long	2, 4, 6, 8, 10, 12, 14, 16, 18	1	30	3 m	Yes
	3, 5, 7, 9, 11	Short	1, 2, 3, 4, 5				
1-type 2	8, 14, 20, 26	Long	2, 4, 6, 8				
	5, 8	Short	1, 2				
1-type 3	8, 14, 20, 26	Long	2, 4, 6, 8,				
	3, 5	Short	1, 2				
2	17	Long	8	0.6, 0.8, 1, 1.2, 1.4, 1.6	30	3 m	Yes
	5	Short	2				
3	17	Long	8	1	5, 10, 15, 20, 25, 30	3 m	Yes
	5	Short	2				
4	17	Long	8	1	30	3,6,9,12,18	Yes
	5	Short	2				

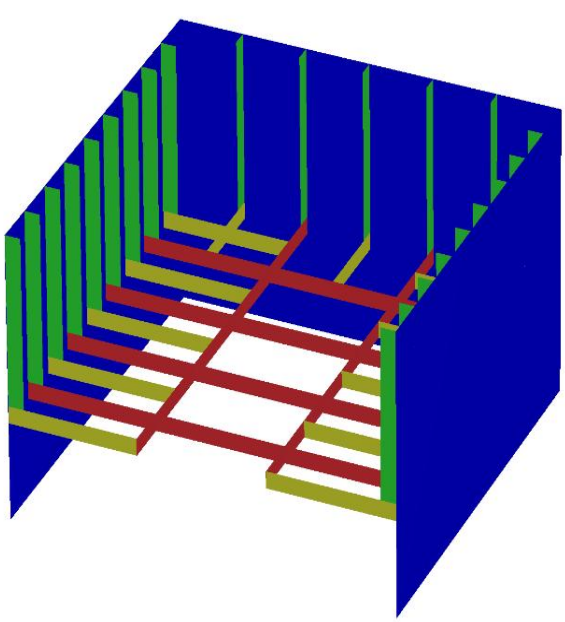

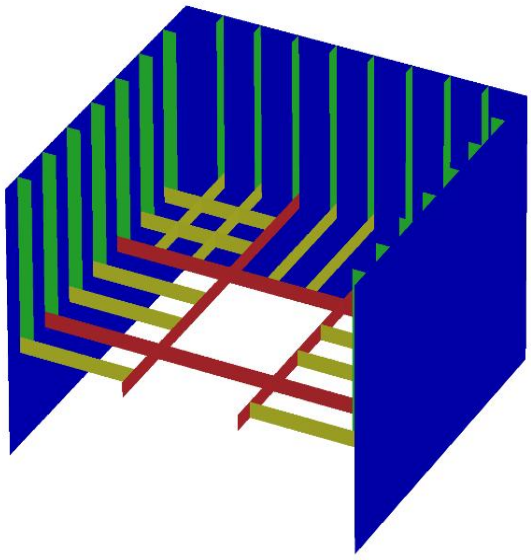

(b)

ISSN 2278-2540 | DOI: 10.51583/IJLTEMAS | Volume XV, Issue I, January 2026

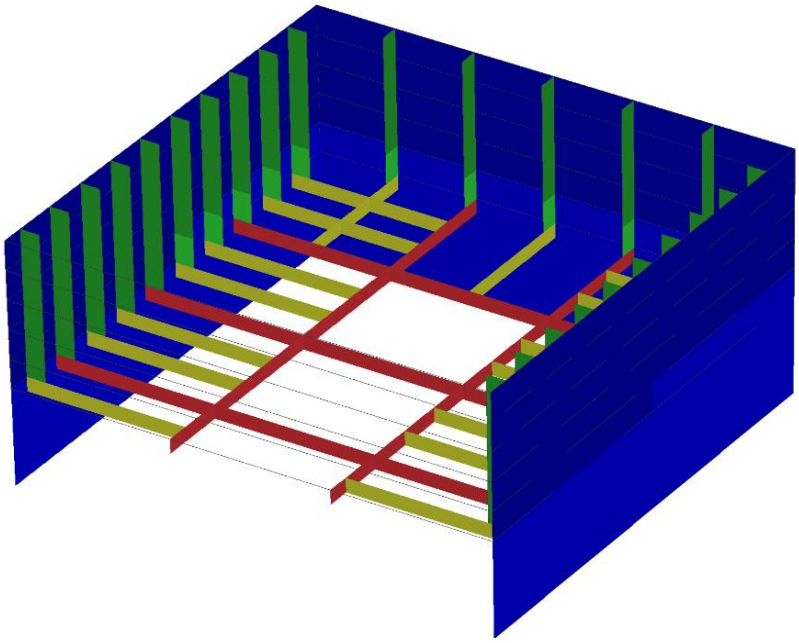

(c)

Figure 4: Three types of excavation design: (a) One rib walls before every cross wall in both directions (b) Two rib walls before every cross wall in both directions (c) Two rib walls before every cross wall in long direction and One rib wall before every cross wall in short direction

Result and analysis

Effect of the number of buttress walls and cross walls on designs

Figure 5 shows the maximum wall deflection in a long direction for different number of buttress walls in both directions for type 1, 2, and 3. The number of buttress walls in short direction did not influence the deflection in long direction in all design types.

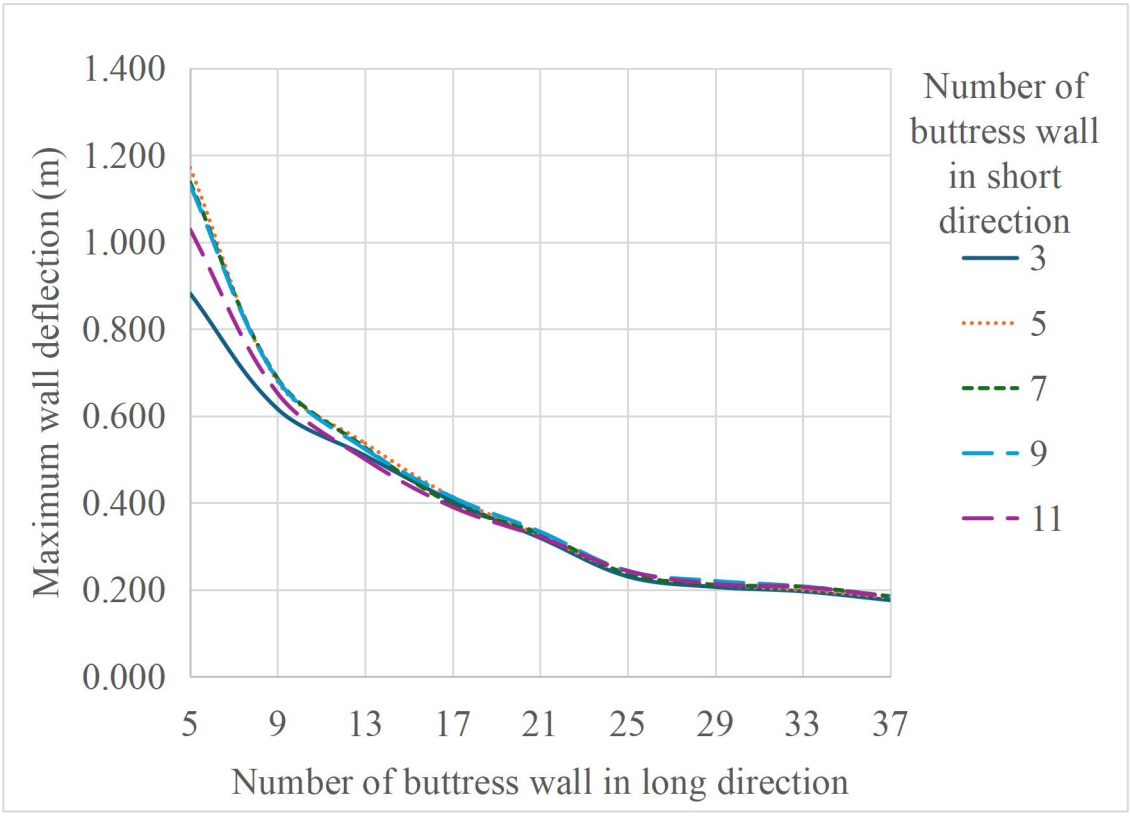

(a)

ISSN 2278-2540 | DOI: 10.51583/IJLTEMAS | Volume XV, Issue I, January 2026

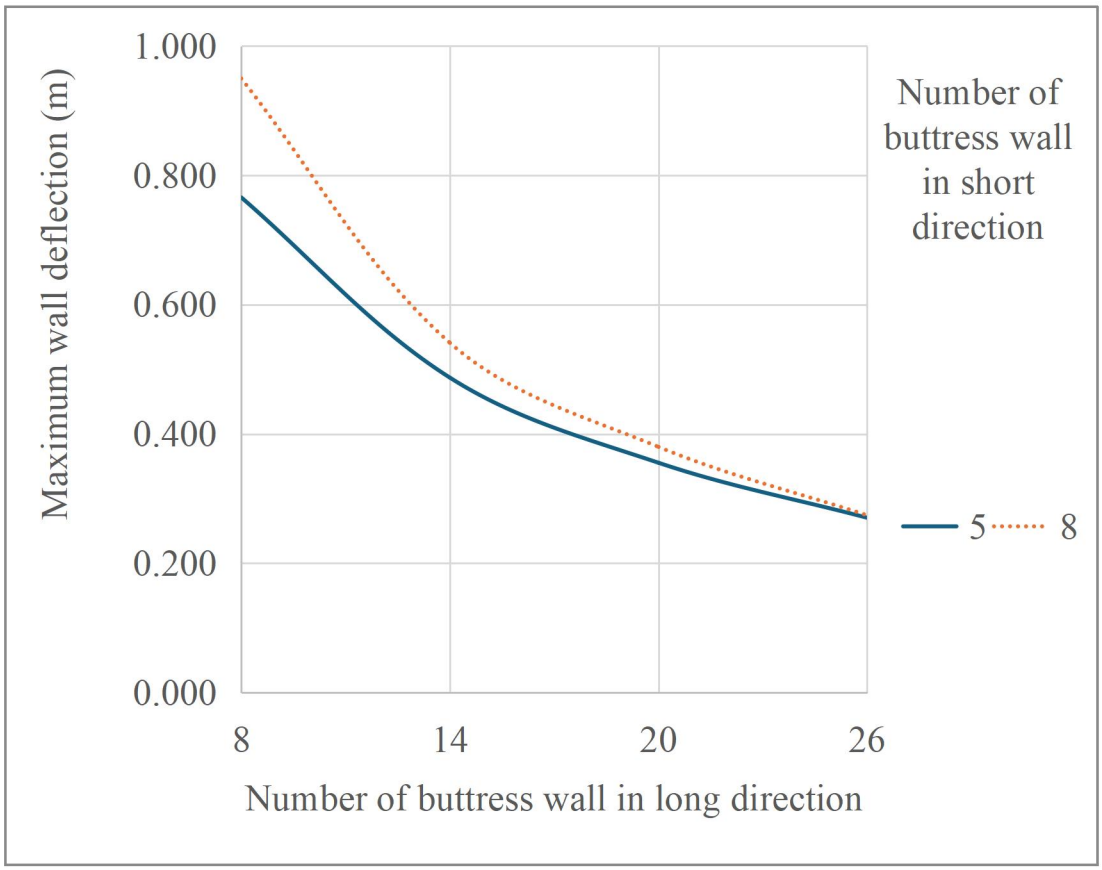

(b)

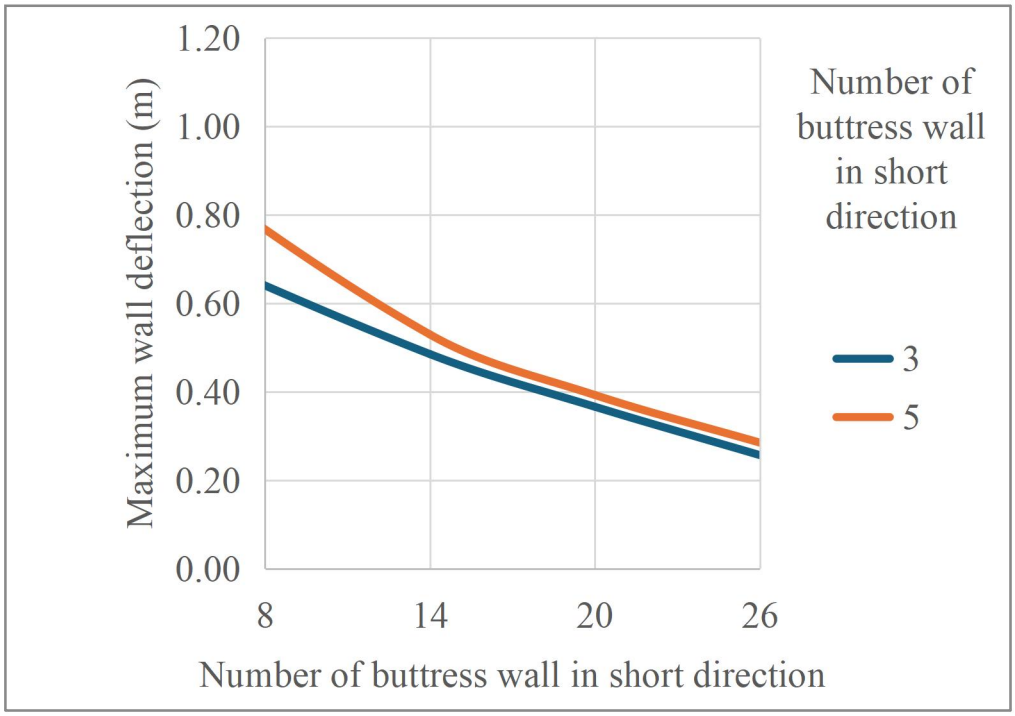

(c)

Figure 5: The maximum wall deflection in a long direction for different number of buttress walls in both directions: (a) type 1 (b) type 2 (c) type 3

From Figure 5, when the number of buttress walls is increased in long direction, the maximum wall deflection in long direction decreased and decreased until the number of buttress walls equals 20, after that, it goes

ISSN 2278-2540 | DOI: 10.51583/IJLTEMAS | Volume XV, Issue I, January 2026

constant as well. Figure 6 shows the maximum ground settlement in a long direction for different number of cross walls in both directions for type 1, 2 and 3.

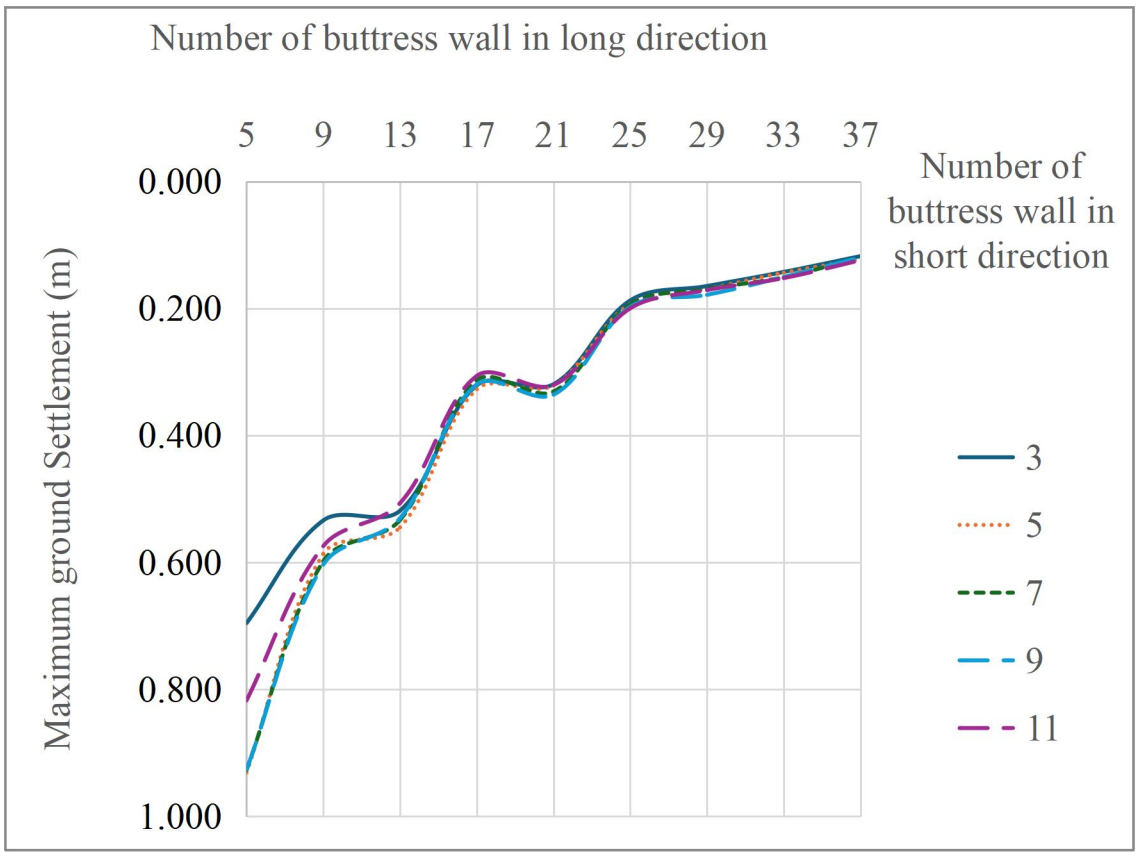

(a)

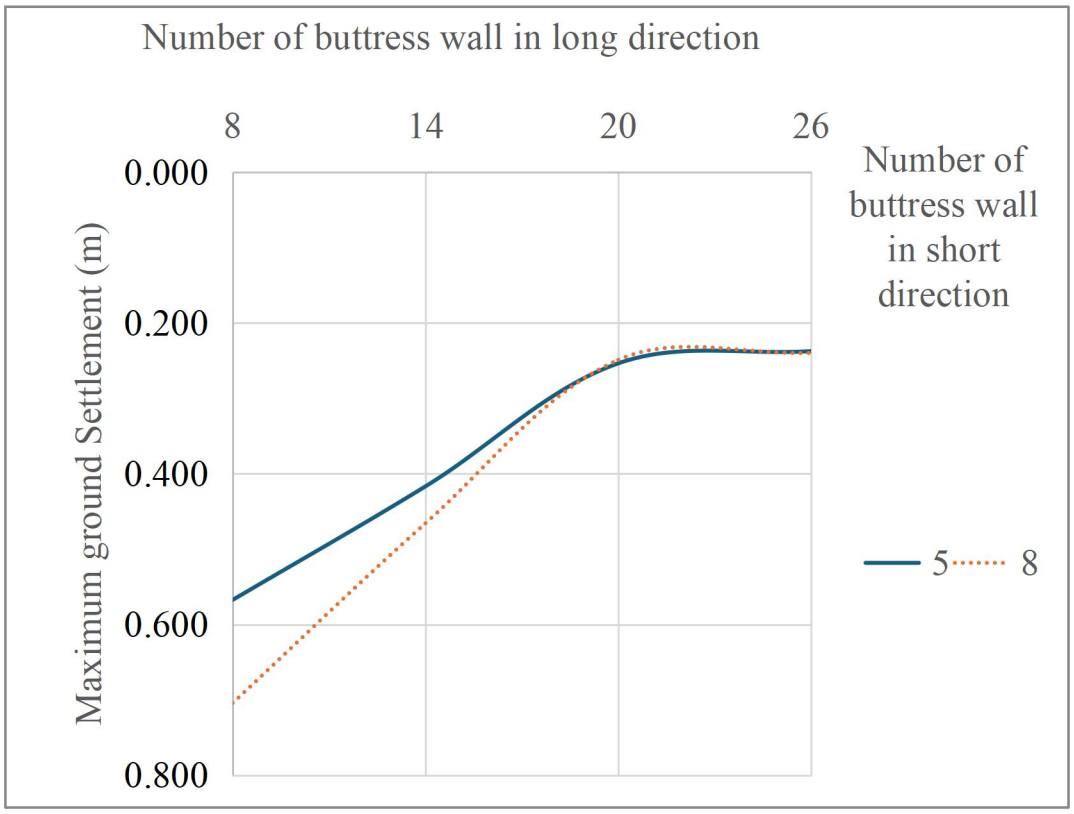

(b)

ISSN 2278-2540 | DOI: 10.51583/IJLTEMAS | Volume XV, Issue I, January 2026

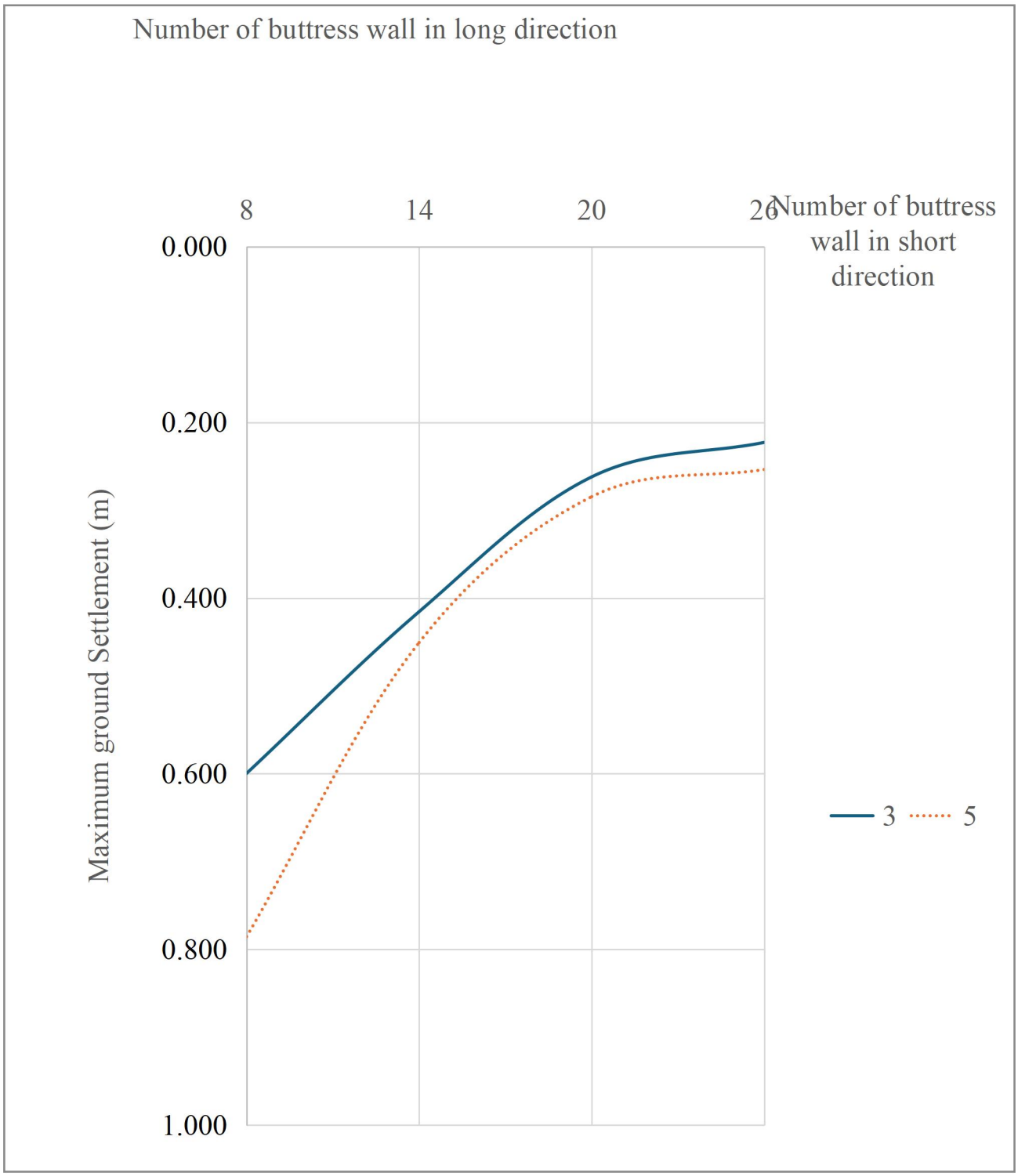

(c)

Figure 6: The maximum ground settlement in a long direction for different number of buttress walls in both directions: (a) type 1 (b) type 2 (c) type 3

From Figure 6, when the number of buttress walls in long direction increased, the maximum ground settlement in the long direction decreased until number of buttress walls equal 20 after that, it goes constant for type 2 and 3. When the number of buttress walls increased, the maximum ground settlement decreased until number of buttress walls equal 25 in type 1. The optimum number of buttress walls in long direction are between 9 to 17, 14 to 20 and 14 to 20 for type 1, 2, and 3, respectively. Figure 7 shows the maximum wall deflection in short direction for different number of buttress walls in both directions for type 1.

ISSN 2278-2540 | DOI: 10.51583/IJLTEMAS | Volume XV, Issue I, January 2026

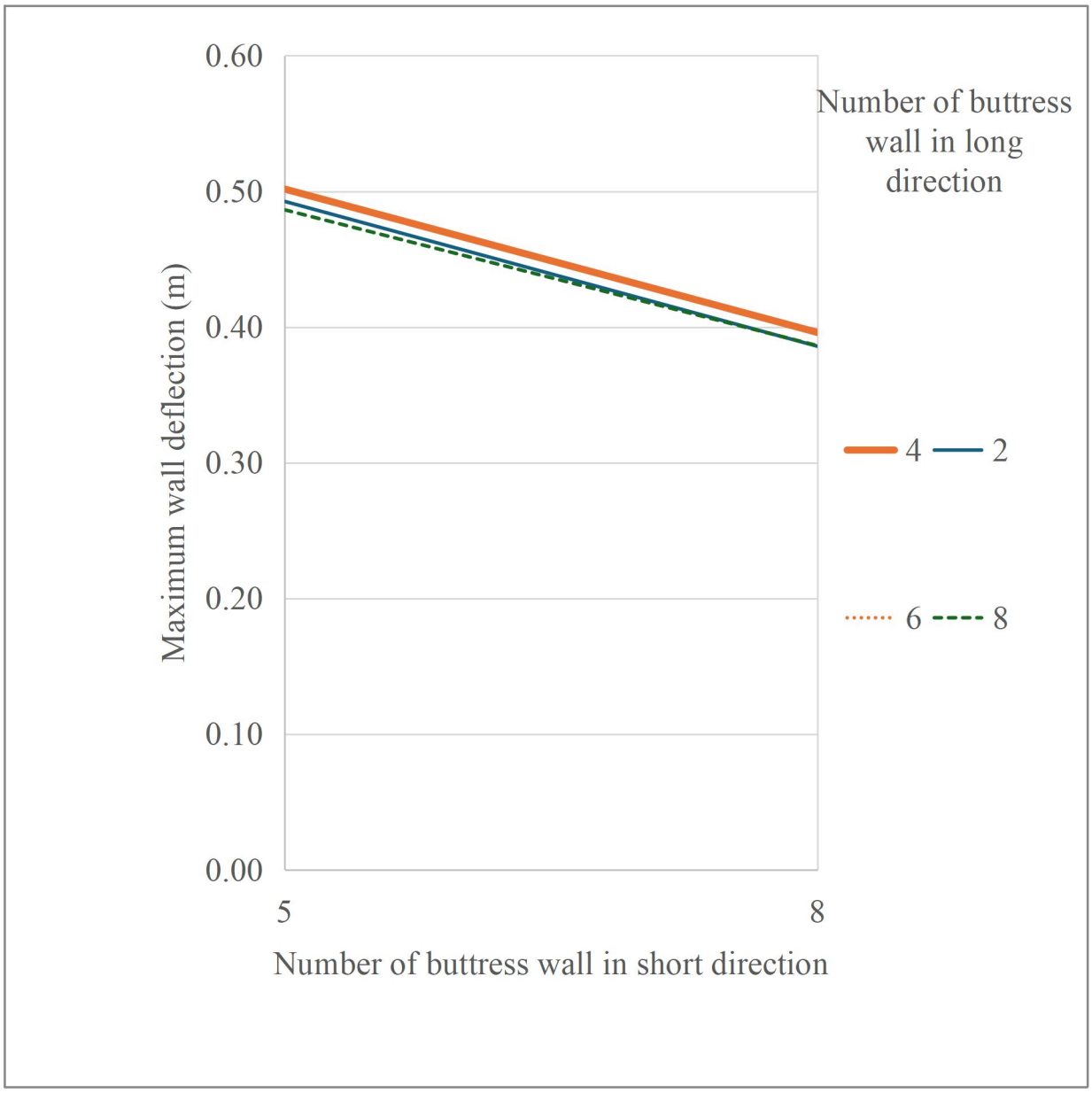

Figure 7: The maximum wall deflection in a short direction for different number of cross walls in both directions (type 2)

It is noted from Figure 11 that when the number of buttress walls in short direction increased, the maximum wall deflection in short direction decreased slightly and the number of buttress wall in long direction did not affect the maximum wall deflection in short direction and the effect of number of buttress walls in short direction is small. Due to that the maximum wall deflection in long direction is the control of deformation for the retaining wall system, so the focus on this paper will be in maximum wall deflection for the rest of this paper. According to the effective range of buttress wall in long direction, the number of cross walls between 4 to 8 and 4 to 6 for type 1 and type 2 respectively. In the same time, the difference of the number of buttress walls between type 1 and 2 is small. On the other hand, the number of buttress walls in short direction has small effect on wall deformation. As result, the type 3 will be optimum design to different type in terms of maximum wall deflection and maximum ground settlement.

Effect of thickness of the cross wall and buttress wall

The excavation model with four cross walls in a long direction and one cross wall in a short direction (type 2)

for the rest of the paper is chosen to investigate the thickness of the cross wall and buttress wall. The thickness of the buttress wall and the cross wall vary from 0.6 m to 1.6 m with 0.2 m increments, as shown in Table 2.

ISSN 2278-2540 | DOI: 10.51583/IJLTEMAS | Volume XV, Issue I, January 2026

Figure 8 shows the maximum wall deflection for different thicknesses for long and short directions respectively. Figure 9 shows the maximum ground settlement for different thicknesses for long and short directions respectively.

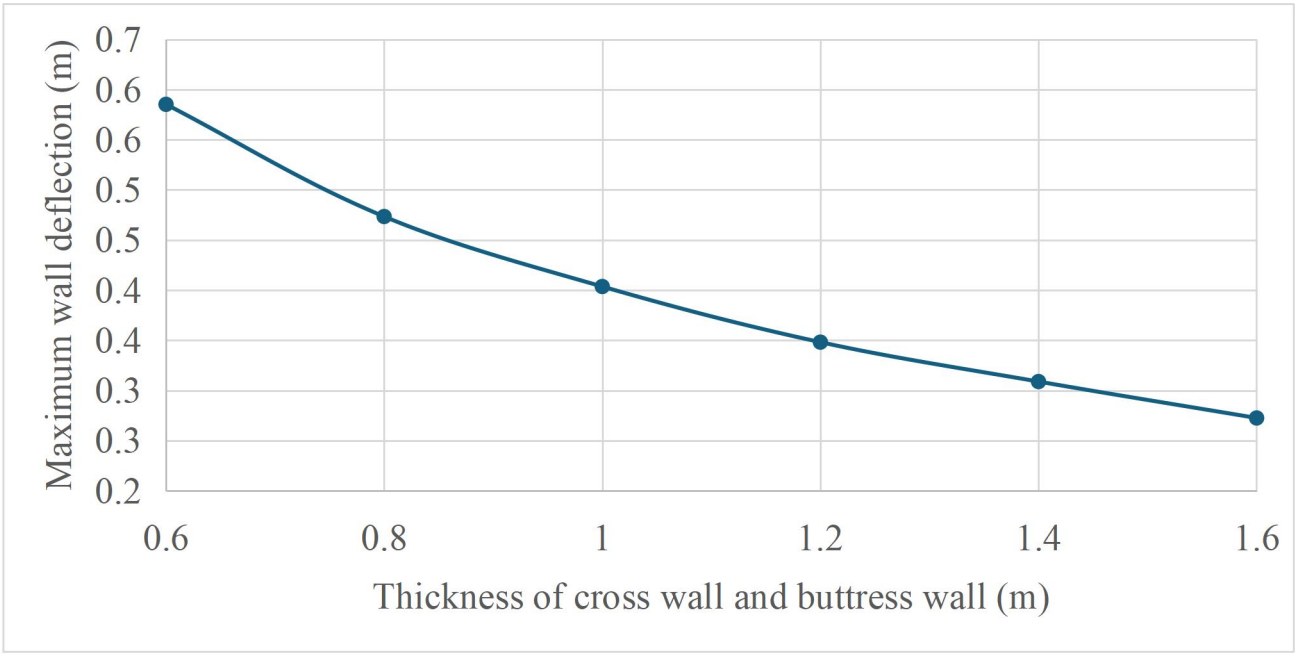

(a)

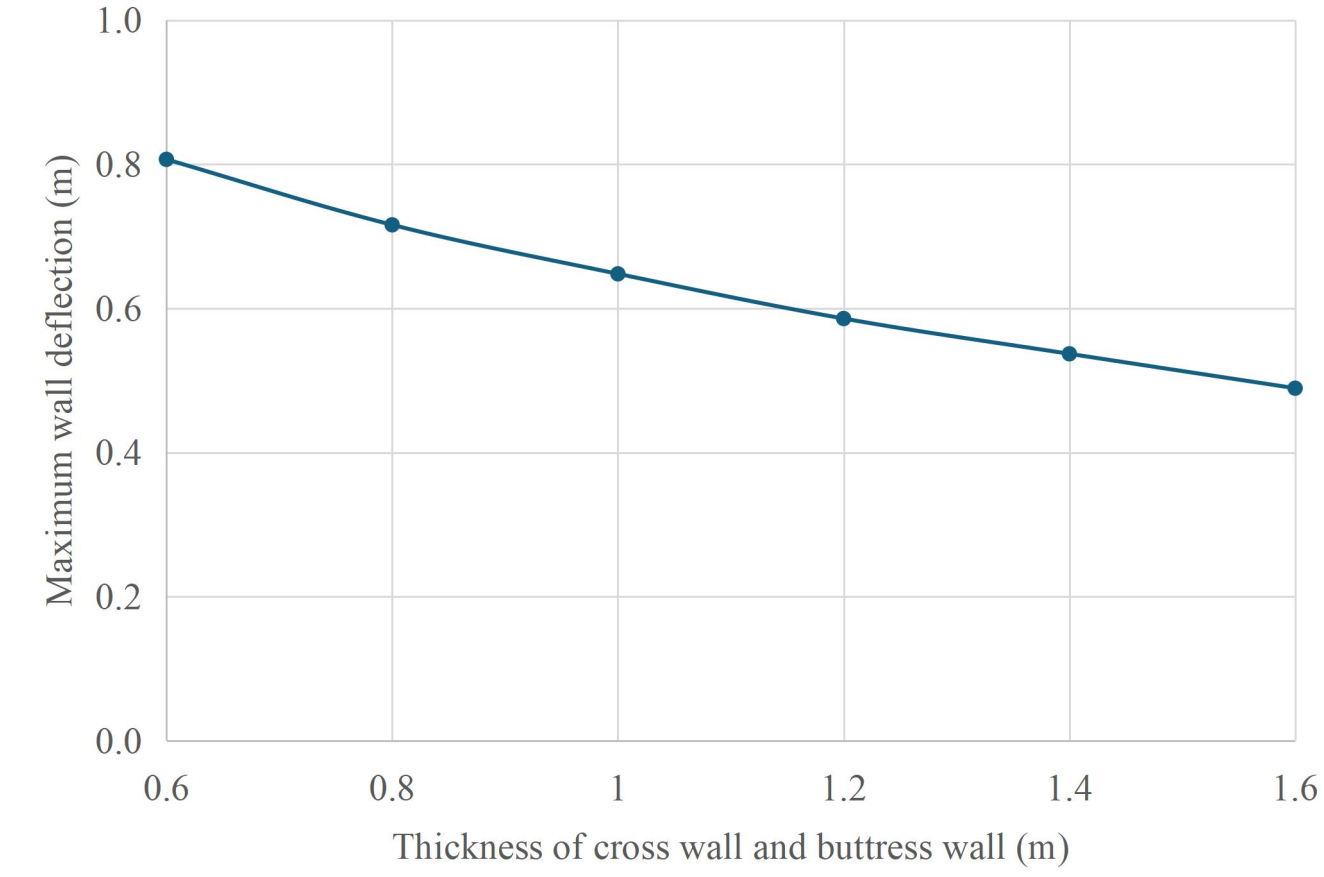

Figure 8: The maximum wall deflection on different thickness of cross wall and buttress wall all and buttress wall (a) long direction (b) short direction

ISSN 2278-2540 | DOI: 10.51583/IJLTEMAS | Volume XV, Issue I, January 2026

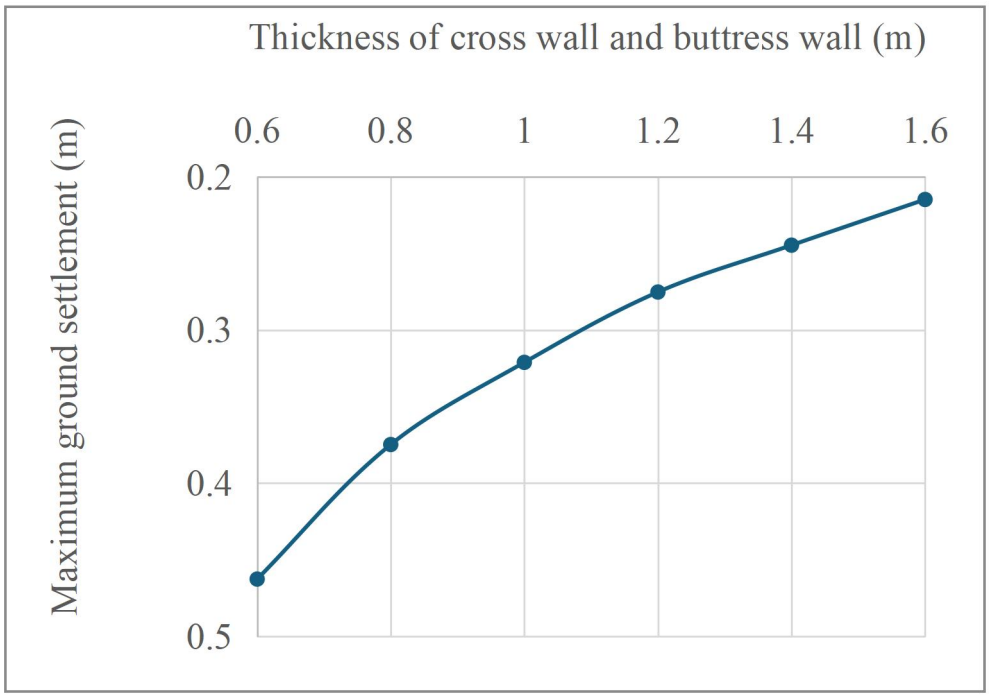

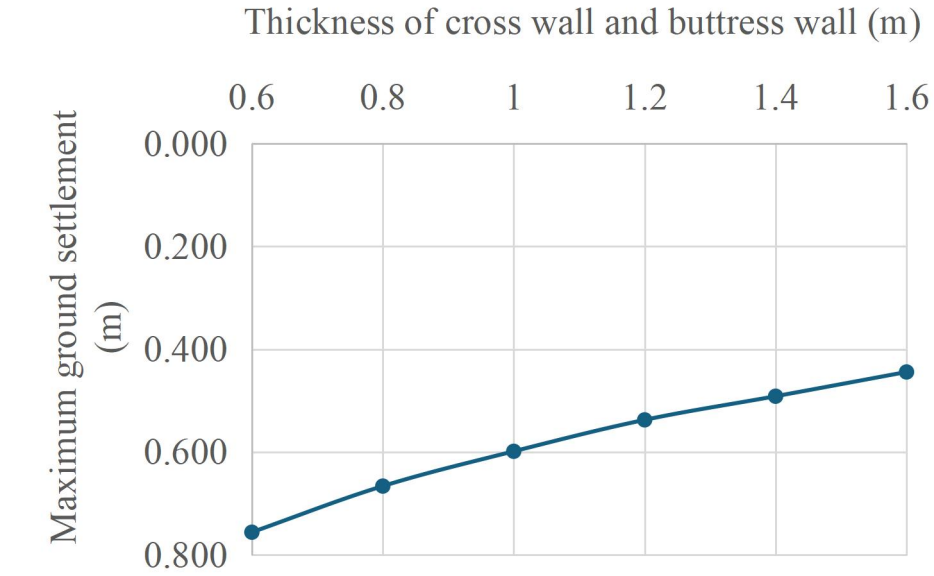

(a)

b)

Figure 9: The maximum ground settlement on different thickness of cross wall and buttress wall: (a) long direction (b) short direction

It is noted that when the thickness of the cross wall and buttress wall increased, the maximum wall deflection and maximum ground settlement decreased in both directions. When the cross wall and buttress wall thickness changed from 0.6 m to 1.2 m, the maximum wall deflection decreased around 40% and 28% of the maximum wall deflection in long and short directions respectively. When the cross wall and buttress wall thickness increased from 0.6 m to 1.2 m, The maximum ground settlement is decreased by 41% and 29% in long and short directions respectively. The increase in buttress wall and cross wall thickness plays a main role in minimizing wall deflection and ground settlement. However, it is not a sufficient solution because it is almost constant when the wall thickness is more than 1.4 m and it is not economic according to ratio of wall deflection and ground settlement to volume of concrete.

ISSN 2278-2540 | DOI: 10.51583/IJLTEMAS | Volume XV, Issue I, January 2026

Effect of height of buttress wall

The height of buttress wall is varied from 5 m to 30 m with 5 m increments as shown in Table 2. Figure 10 shows the maximum wall deflection at different heights of the buttress wall in long and short directions, respectively. Figure 11 shows the maximum ground settlement on the different heights of the buttress wall in long and short directions respectively.

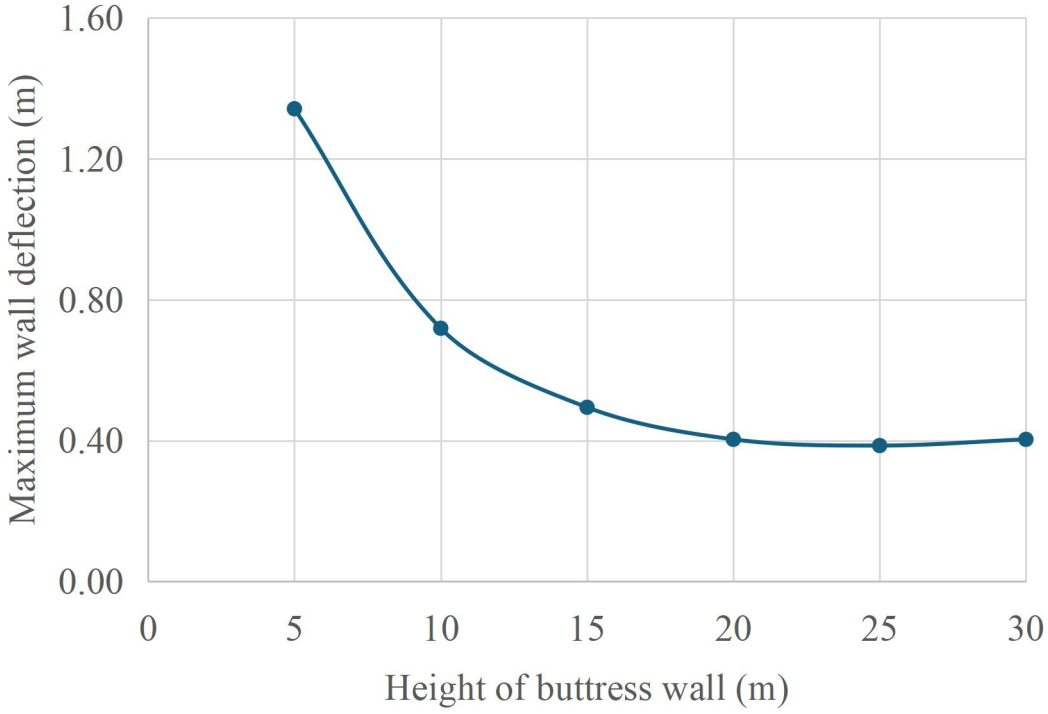

(a)

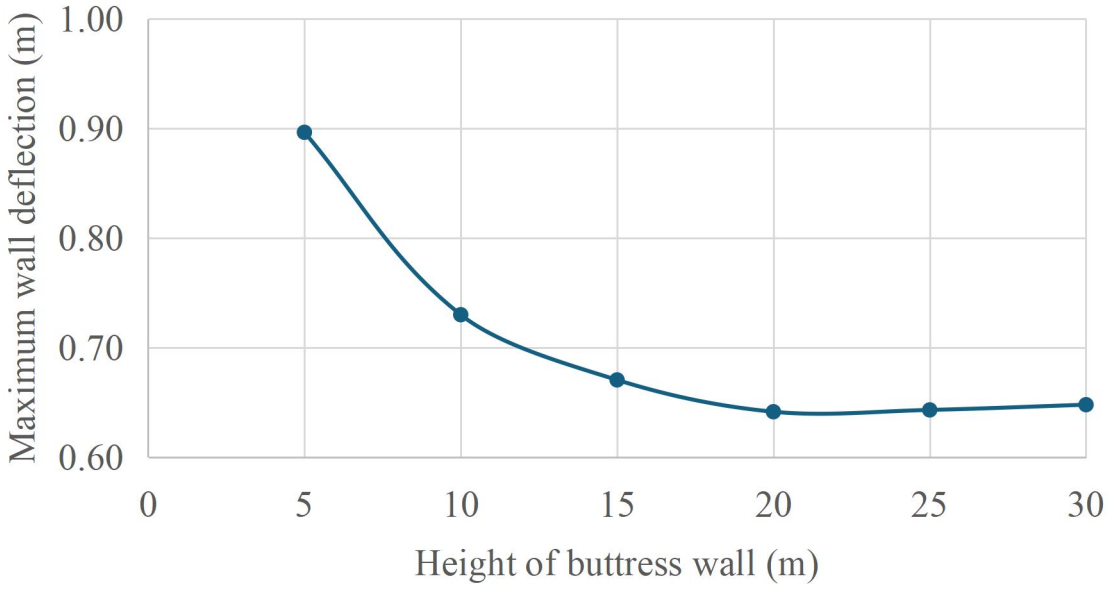

(b)

Figure 10: The maximum wall deflection on different heights of the buttress wall: (a) long direction (b) short direction

ISSN 2278-2540 | DOI: 10.51583/IJLTEMAS | Volume XV, Issue I, January 2026

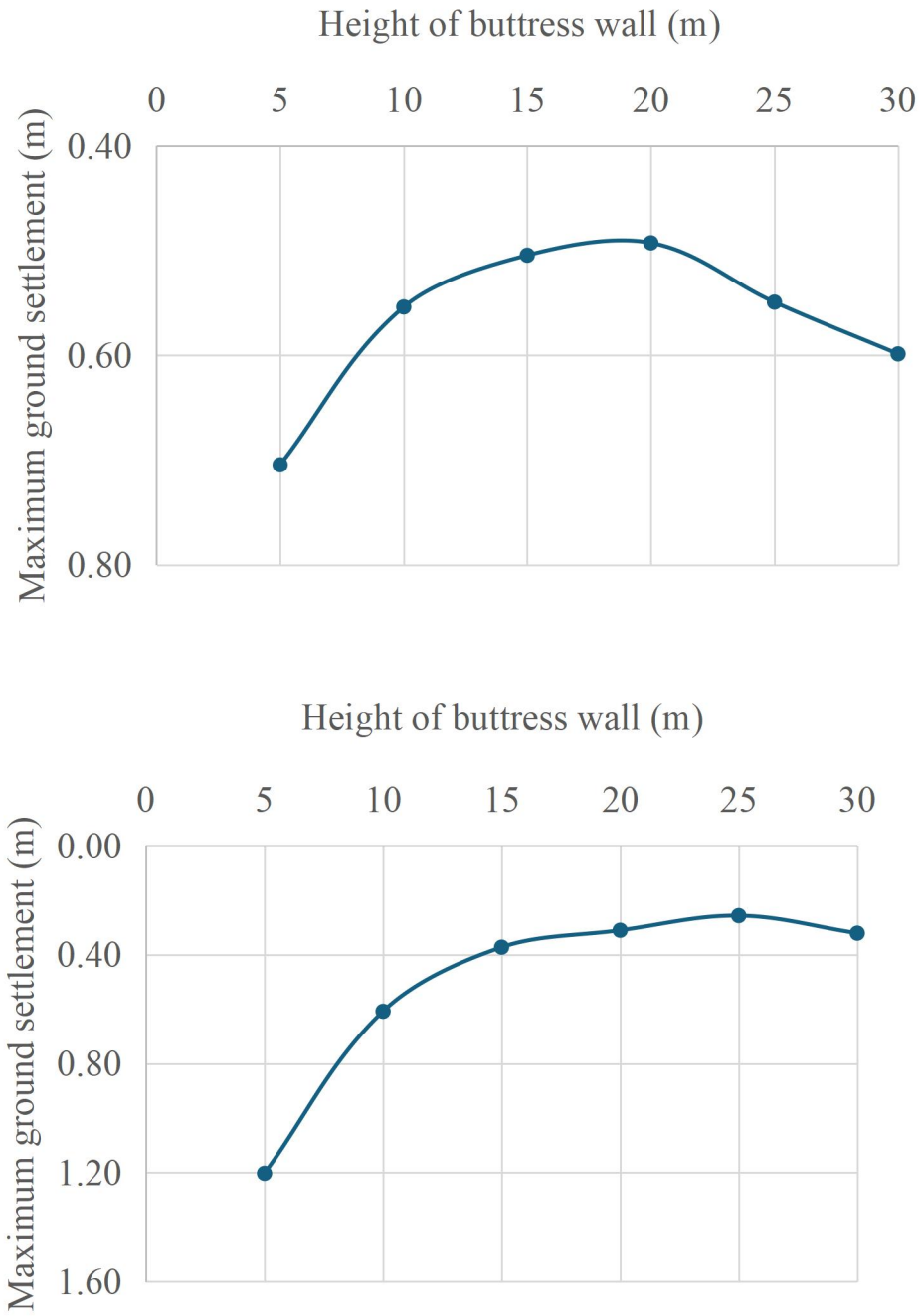

Figure 11: The maximum ground settlement on different heights of the buttress wall: (a) long direction (b) short direction

From Figure 10 and Figure 11, it is noted that the maximum wall deflection and ground settlement are constant when the height of the buttress wall height is from 20 to 30 m in both directions. The decreasing in buttress wall height from 20 to 5 m is leading to an increase dramatically in maximum wall deflection and ground settlement and this is clear in the long direction more than the short direction because the number of buttress walls in long direction.

Effect of the height of the cross wall

Figure 12 shows the maximum wall deflection on different heights of the buttress wall in long and short directions respectively. Figure 13 shows the maximum ground settlement on different heights of the buttress wall in long and short directions respectively.

ISSN 2278-2540 | DOI: 10.51583/IJLTEMAS | Volume XV, Issue I, January 2026

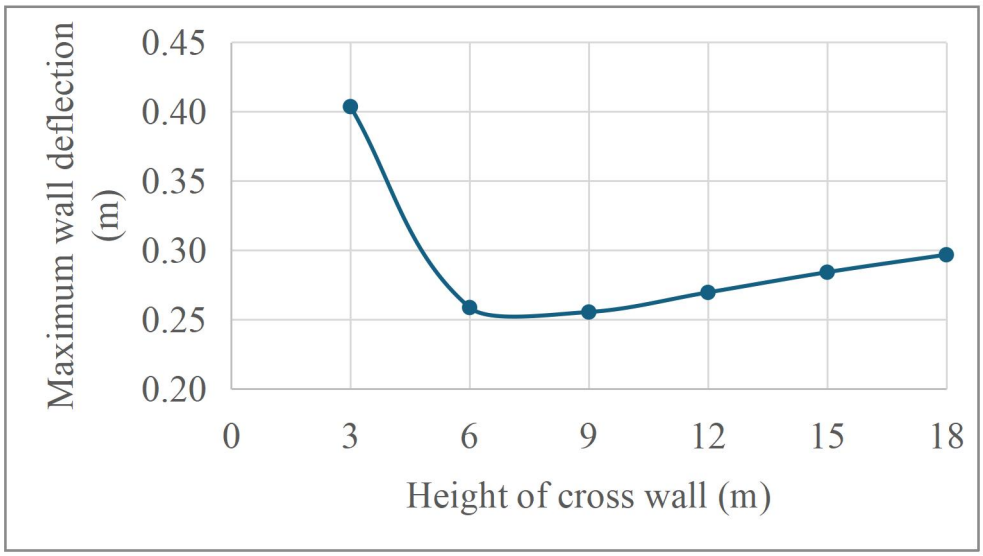

(a)

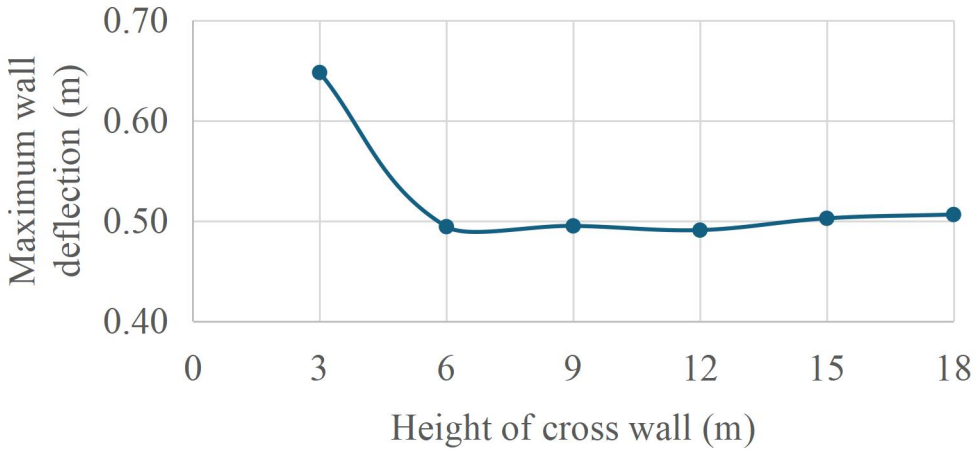

(b)

Figure 12: The maximum wall deflection on different heights of the cross wall: (a) long direction (b) short direction

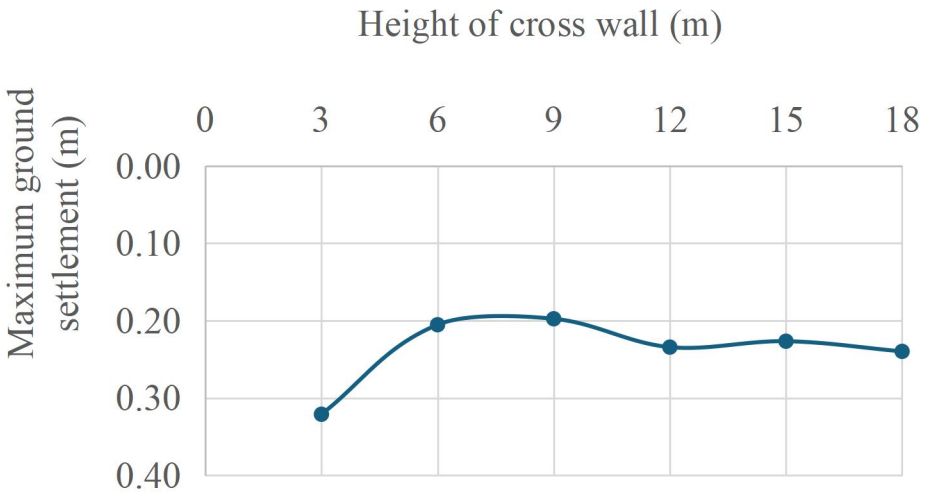

ISSN 2278-2540 | DOI: 10.51583/IJLTEMAS | Volume XV, Issue I, January 2026

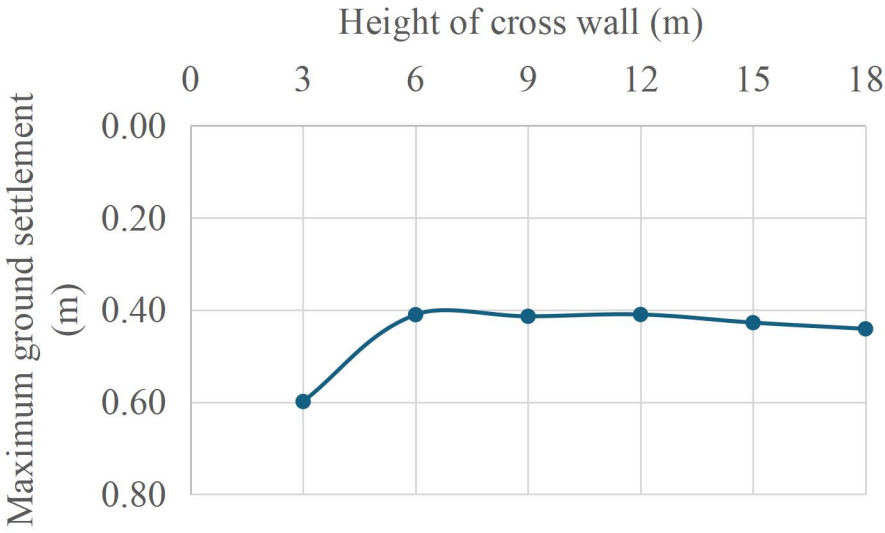

Figure 13: The maximum ground settlement on different heights of the cross wall: (a) long direction (b) short direction

It is noted that the maximum wall deflection and the maximum ground settlement are decreased when the height of the cross wall is increased until it is equal to 6 m. After that, it goes constant as shown in Figure 12 and Figure 13. Also, the maximum wall deflection of 6 m cross wall high is decreased by about 37 % and 32% of the maximum wall deflection of 3 m cross wall high in long and short directions respectively. The maximum ground settlement of 6 m cross wall high is decreased about 37 % and 9% of maximum ground settlement of 3 m cross wall high.

The profile of the diaphragm wall and ground settlement

The location of maximum wall deflection and maximum ground settlement in the short direction is in the middle of the short direction and the location of maximum wall deflection and maximum ground settlement in the long direction is in the middle of the long direction. Also, all the wall deformation is cantilever shape with a small transition at the toe of the diaphragm wall for both directions. The ground settlement deformation is spandrel type and the shape of wall deformation and ground settlement is expected to occur [1] for all series in Table 2.

CONCLUSIONS

This paper presents a series of three-dimensional finite element analyses to optimum design for strut-free retaining wall system and effective range the number of buttress walls and cross walls, the effect of thickness of the cross wall, height of buttress wall and height of the cross wall to understand deformation control mechanisms of excavation. The following conclusions can be presented:

1- The optimum number of buttress walls in long direction are between 9 to 17, 14 to 20 and 14 to 20 for type 1, 2, and 3, respectively.
2- The effect of the number of buttress walls plays a significant role in controlling the deformation characteristic of the excavation system in the long but not in the short direction. This requires the use of additional procedures to control in the short direction.
3- the type 3 will be optimum design to different type in terms of maximum wall deflection and maximum ground settlement.
4- The decrease in the number of cross walls and buttress walls decreased the stiffness of the excavation project and did not affect the deformation characteristic of the excavation system [31, 32].
5- Effect of thickness of the cross wall and buttress wall is between 0.6 m and 1 m.
6- When the height of the buttress walls is from 20 to 30 m, the retaining system characteristics are constant. The decreasing in buttress wall height from 20 to 5 m is leading to an increase dramatically in maximum wall deflection and ground settlement.

ISSN 2278-2540 | DOI: 10.51583/IJLTEMAS | Volume XV, Issue I, January 2026

7- When the height of the cross walls is from 6 to 9 m, the retaining system characteristics are constant. The decreasing in cross wall height from 6 to 3 m is leading to an increase in maximum wall deflection and ground settlement.

REFERENCES

1. A. Lim and C.-Y. Ou, "Case Record of a Strut-free Excavation with Buttress Walls in Soft Soil," in Proceedings of the 2nd International Symposium on Asia Urban GeoEngineering, 2018: Springer, pp. 142–154.
2. C. Ou, Y. Lin, and P. Hsieh 2006. Case record of an excavation with cross walls and buttress walls. Journal of GeoEngineering. 1, 2, 79–87.
3. C.-Y. Ou, F.-C. Teng, R. B. Seed, and I.-W. Wang 2008. Using buttress walls to reduce excavation-induced movements. Proceedings of the Institution of Civil Engineers-Geotechnical Engineering. 161, 4, 209–222.
4. C.-Y. Ou, P.-G. Hsieh, and Y.-L. Lin 2011. Performance of excavations with cross walls. Journal of Geotechnical and Geoenvironmental Engineering. 137, 1, 94–104.
5. P.-G. Hsieh, C.-Y. Ou, and Y.-L. Lin 2013. Three-dimensional numerical analysis of deep excavations with cross walls. Acta Geotechnica. 8, 33–48.
6. C.-Y. Ou, P.-G. Hsieh, and Y.-L. Lin 2013. A parametric study of wall deflections in deep excavations with the installation of cross walls. Computers and Geotechnics. 50, 55–65.
7. P.-G. Hsieh, C.-Y. Ou, Y.-K. Lin, and F.-C. Lu 2015. Lessons learned in design of an excavation with the installation of buttress walls. Journal of GeoEngineering. 10, 2, 63–73.
8. P.-G. Hsieh, C.-Y. Ou, and W.-H. Hsieh 2016. Efficiency of excavations with buttress walls in reducing the deflection of the diaphragm wall. Acta Geotechnica. 11, 1087–1102.
9. A. Lim and C.-Y. Ou 2018. Performance and three-dimensional analyses of a wide excavation in soft soil with strut-free retaining system. International Journal of Geomechanics. 18, 9, 05018007.
10. C. Ou, A. Lim, P. Hsieh, and S. Chien, "A study of a strut-free excavation system in deep excavations," in Geotechnical Aspects of Underground Construction in Soft Ground: CRC Press, 2021, pp. 365–370.
11. G. Zheng, X. He, H. Zhou, Y. Diao, Z. Li, and X. Liu 2022. Performance of inclined-vertical framed retaining wall for excavation in clay. Tunnelling and Underground Space Technology. 130, 104767.
12. S.-H. Wu, J. Ching, and C.-Y. Ou 2013. Predicting wall displacements for excavations with cross walls in soft clay. Journal of Geotechnical and Geoenvironmental Engineering. 139, 6, 914–927.
13. W. Zhang, A. T. Goh, and F. Xuan 2015. A simple prediction model for wall deflection caused by braced excavation in clays. Computers and Geotechnics. 63, 67–72.
14. A. Goh, F. Zhang, W. Zhang, Y. Zhang, and H. Liu 2017. A simple estimation model for 3D braced excavation wall deflection. Computers and Geotechnics. 83, 106–113.
15. G. Zheng, Z.-p. Liu, H.-z. Zhou, X.-p. He, and Z.-y. Guo 2022. Behaviour of an outward inclined-vertical framed retaining wall of an excavation. Acta Geotechnica. 17, 12, 5521–5532.
16. C. Moormann 2004. Analysis of wall and ground movements due to deep excavations in soft soil based on a new worldwide database. Soils and foundations. 44, 1, 87–98.
17. Y. Tan, D. Fan, and Y. Lu 2022. Statistical analyses on a database of deep excavations in Shanghai soft clays in China from 1995–2018. Practice Periodical on Structural Design and Construction. 27, 1, 04021067.
18. C.-Y. Ou, Fundamentals of Deep Excavations. CRC Press, 2021.
19. P. Vermeer and M. Wehnert, "Beispiele von FE-Anwendungen–Man lernt nie aus," in Tagungsband zum Workshop'FEM in der Geotechnik–Qualität, Prüfung, Fallbeispiele, Hamburg, 2005, pp. 101–119.
20. C.-Y. Ou, Deep excavation: Theory and practice. CRC Press, 2014.
21. T. Schanz, P. Vermeer, and P. Bonnier 1999. Formulation and verification of the Hardening-Soil model. Beyond 2000 in Computational Geotechnics Brinkgreveed Rotterdam Balkema. 281–290.
22. M. Calvello and R. J. Finno 2004. Selecting parameters to optimize in model calibration by inverse analysis. Computers and Geotechnics. 31, 5, 411–425.
23. M. Bolton 1986. The strength and dilatancy of sands. Geotechnique. 36, 1, 65–78.
24. A. Lim, C.-Y. Ou, and P.-G. Hsieh 2010. Evaluation of clay constitutive models for analysis of deep excavation under undrained conditions. Journal of GeoEngineering. 5, 1, 9–20.

ISSN 2278-2540 | DOI: 10.51583/IJLTEMAS | Volume XV, Issue I, January 2026

25. M. D. James and C. Chin-Yung 1970. Nonlinear analysis of stress and strain in soils. Journal of the Soil Mechanics and Foundations Division. 96, 5, 1629–1653.
26. A. Lim, C.-Y. Ou, and P.-G. Hsieh 2020. A novel strut-free retaining wall system for deep excavation in soft clay: numerical study. Acta Geotechnica. 15, 6, 1557–1576.
27. A. Lim and C.-Y. Ou 2017. Stress paths in deep excavations under undrained conditions and its influence on deformation analysis. Tunnelling and Underground Space Technology. 63, 118–132.
28. American Concrete Institute ACI 318-19, "Building Code Requirements for Structural Concrete," ed, 2022.
29. Bentley, "Material Models Manual of PLAXIS CONNECT Edition V21.01," ed, 2021.
30. C.-Y. Ou, J.-T. Liao, and H.-D. Lin 1998. Performance of diaphragm wall constructed using top-down method. Journal of Geotechnical and Geoenvironmental Engineering. 124, 9, 798–808.
31. L. S. Bryson and D. G. Zapata-Medina 2012. Method for estimating system stiffness for excavation support walls. Journal of Geotechnical and Geoenvironmental Engineering. 138, 9, 1104–1115.
32. S. Lam, S. Haigh, and M. Bolton 2014. Understanding ground deformation mechanisms for multi-propped excavation in soft clay. Soils and Foundations. 54, 3, 296–312.